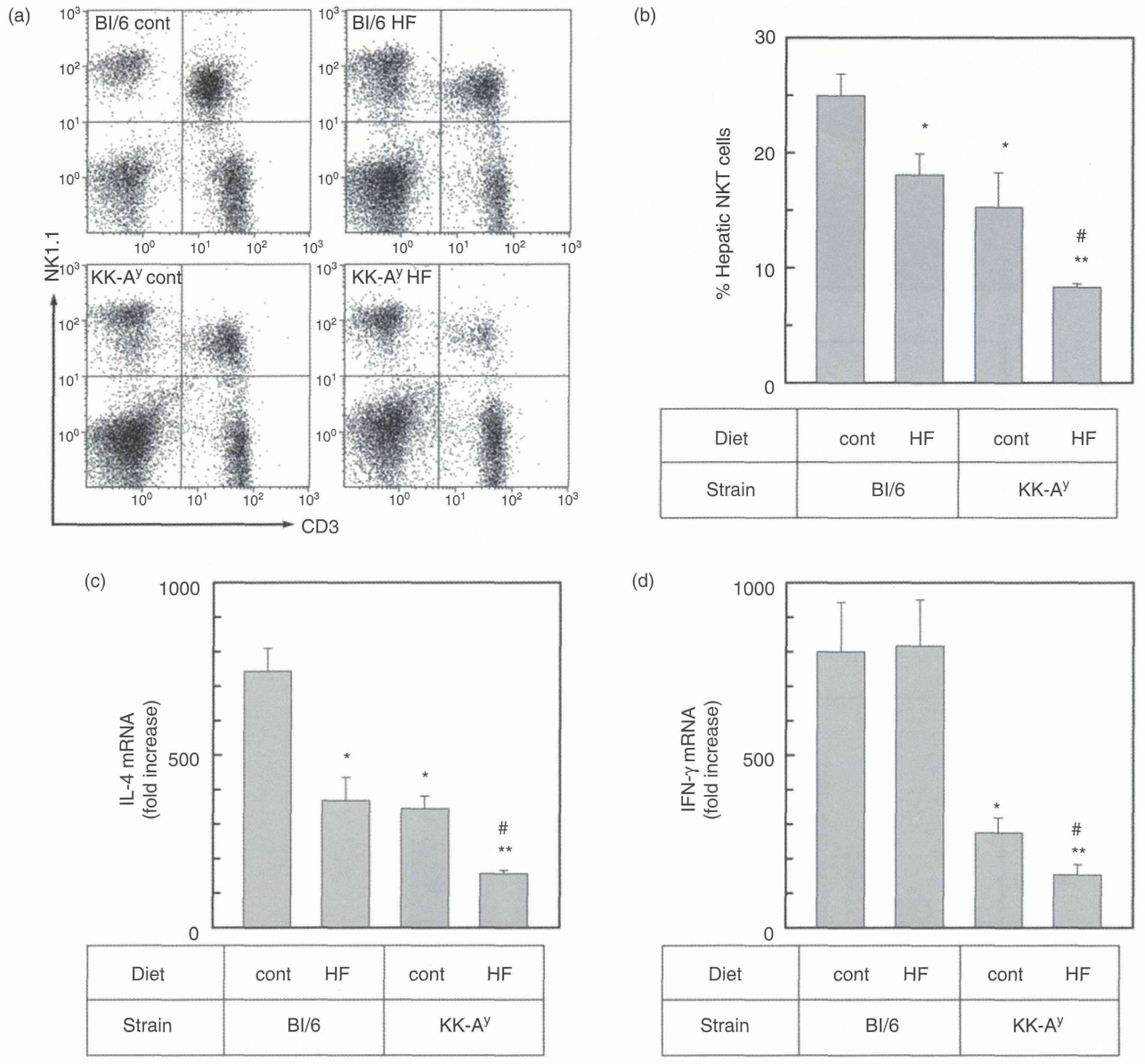

Figure 3 Hepatic NKT cells are progressively depleted in KK-A^y mice following HF diet feeding. Hepatic NKT cells in both strains of mice fed a HF diet or a control diet for 4 weeks were detected by fluorescence-activated cell sorting analysis. Representative plots from C57Bl/6 fed a control diet (a; left upper panel), C57Bl/6 fed a HF diet (a; right upper panel), KK-A^y fed a control diet (a; left lower panel) and KK-A^y fed a HF diet (a; lower right panel) are shown. Percentages of hepatic NKT cells in each strain following dietary treatment are plotted (b). Peak mRNA levels of IL-4 (at 3 h) and IFN-γ (at 12 h) in the liver after a single injection of GalCer in both strains of mice following 4-week dietary treatment were measured by real time reverse transcription polymerase chain reaction. Average values of fold increase over the control C57Bl/6 levels for IL-4 (c) and IFN-γ (d) are plotted ($n = 5$, mean ± SEM, *$P < 0.05$ vs Bl/6 controls, **$P < 0.05$ vs HF-fed Bl/6, #$P < 0.05$ vs KK-A^y controls, by ANOVA on ranks and Student–Newman–Keuls post-hoc test). HF, high fat; IFN, interferon; IL, interleukin; NKT cells, natural killer T cells; SEM, standard error of the mean.

© 2012 The Japan Society of Hepatology

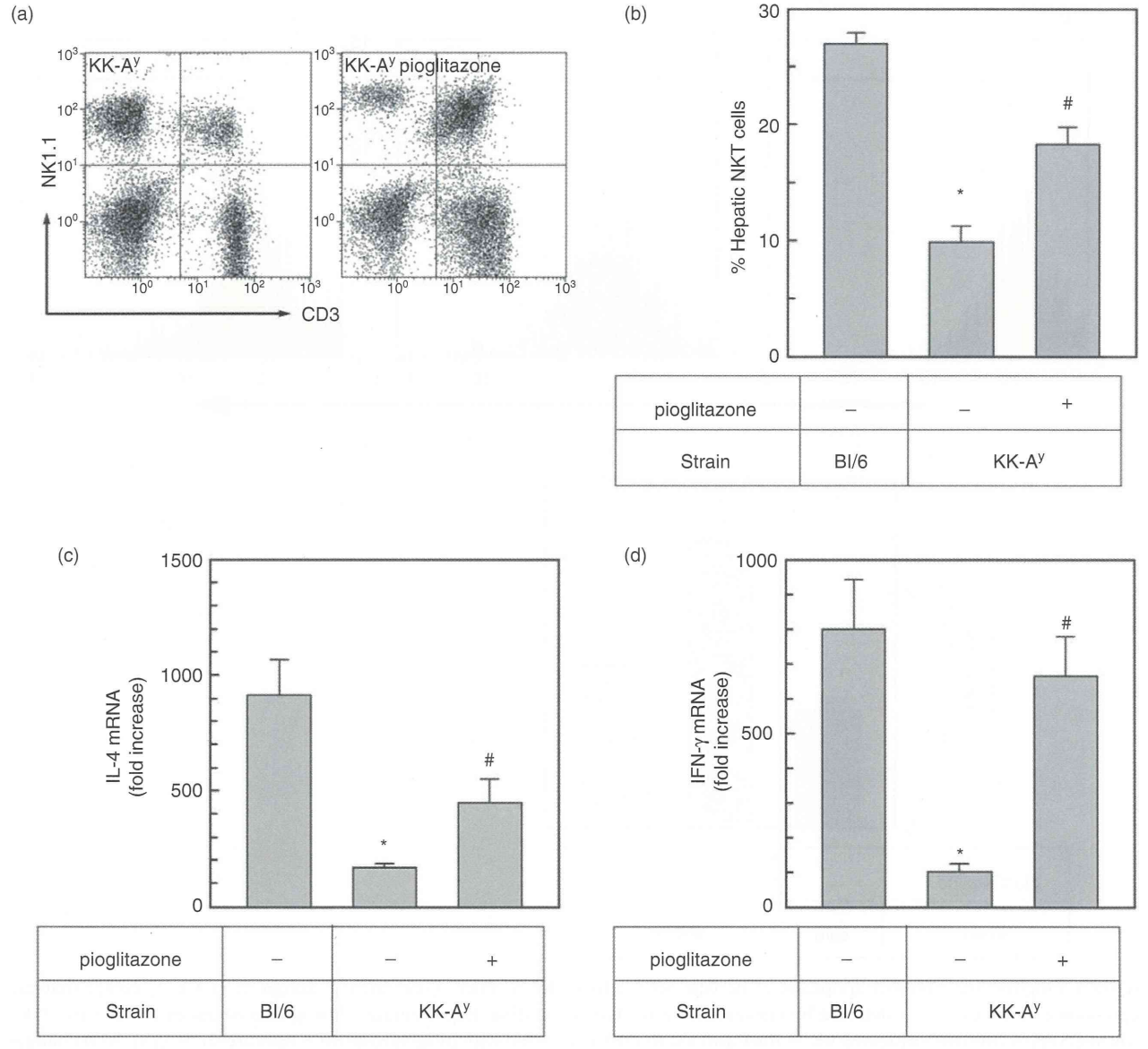

Figure 4 Pioglitazone increases expression of NKT cells in KK-A^y mice before dietary treatment. KK-A^y mice (8 weeks old) were given daily intragastric injection of pioglitazone (25 mg/kg) for 5 days, and hepatic NKT cells were detected by fluorescence-activated cell sorting analysis. Representative plots from control KK-A^y (a; left panel) and KK-A^y pretreated with pioglitazone (a; right panel) are shown. Percentages of hepatic NKT cells in C57Bl/6 control, KK-A^y with/without pioglitazone pretreatment are plotted (b). Peak mRNA levels of IL-4 (at 3 h) and IFN-γ (at 12 h) in the liver after a single injection of GalCer in C57Bl/6 and KK-A^y mice with/without pioglitazone treatment were measured by real time reverse transcription polymerase chain reaction. Average values of fold increase over control, C57Bl/6 levels for IL-4 (c) and IFN-γ (d) are plotted ($n = 5$, mean ± SEM, $^*P < 0.05$ vs Bl/6 controls, $\#P < 0.05$ vs KK-A^y controls, by ANOVA on ranks and Student–Newman–Keuls post-hoc test). IFN, interferon; IL, interleukin; NKT cells, natural killer T cells; SEM, standard error of the mean.

people. This discrepancy most likely indicated that proportional and functional abnormalities in hepatic NKT cells in steatohepatitis cannot be explained simply by leptin-specific mechanisms. Rather, KK-A^y mice showed marked hypoadiponectinemia, and HF diet feeding decreased serum adiponectin levels both in C57Bl/6 and KK-A^y mice (Fig. 2f), the phenomena being related to decreases in hepatic NKT-cell fraction, suggesting that

© 2012 The Japan Society of Hepatology

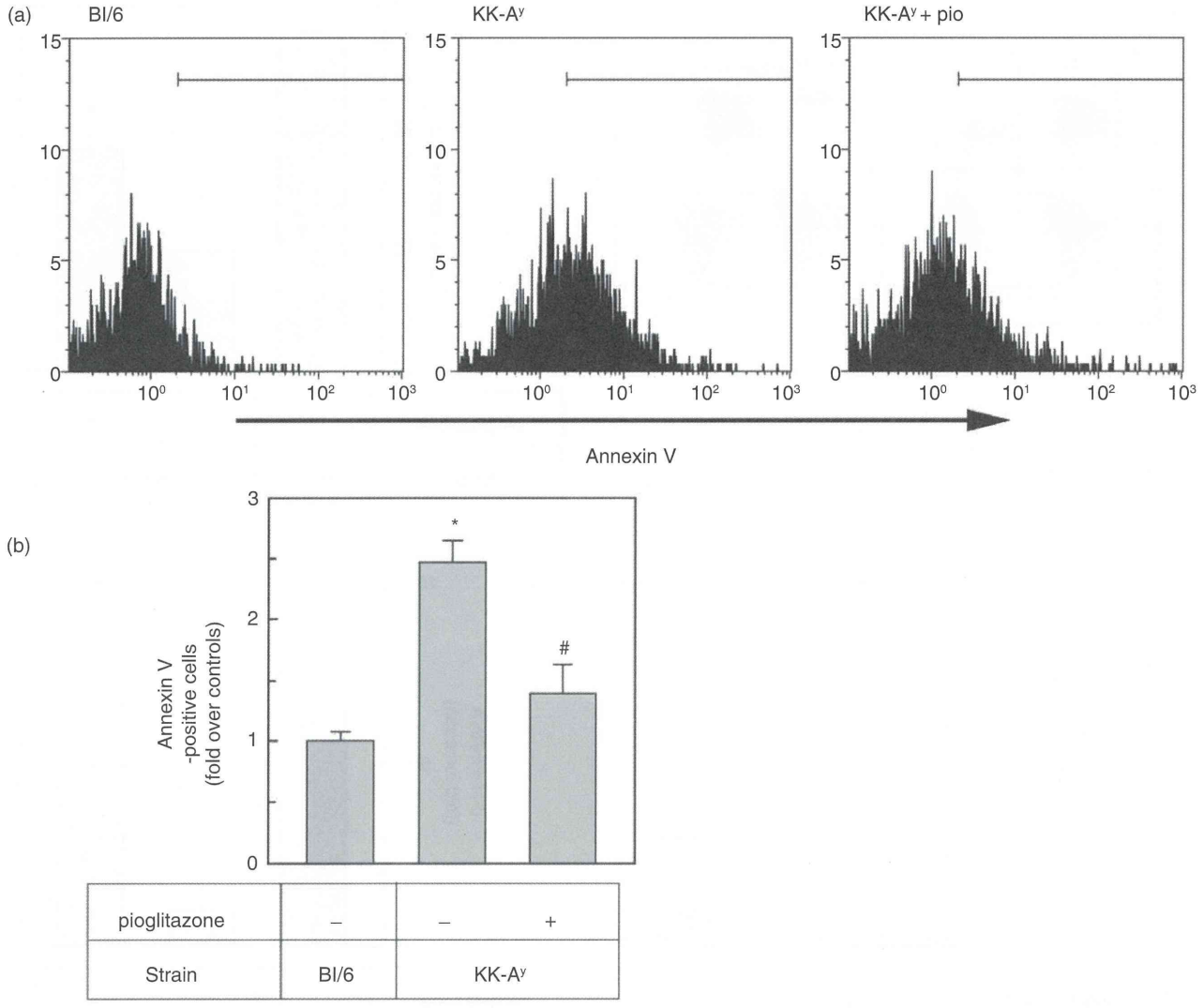

Figure 5 Pioglitazone prevents apoptosis of hepatic NKT cells in KK-A^y mice. Experimental design as in Fig. 4, except that the expression of annexin V was detected by fluorescence-activated cell sorting. Representative histograms of annexin V positive NKT cells in C57Bl/6 controls, untreated KK-A^y mice and KK-A^y mice pretreated with pioglitazone for 5 days are shown (a). Fold changes in annexin V positive NKT cells in these mice are plotted (b; $n = 5$, mean ± SEM, $^*P < 0.05$ vs Bl/6 controls, $\#P < 0.05$ vs KK-A^y controls, by ANOVA on ranks and Student–Newman–Keuls post-hoc test). NKT cells, natural killer T cells; SEM, standard error of the mean.

adiponectin plays a key role in expression and function of hepatic NKT cells.

Peroxisome proliferator-activated receptor-γ is a key nuclear receptor/transcription factor for transcriptional regulation of various genes related to glucose/lipid metabolism, immune responses and tissue repair.[31] Because TZD, synthetic PPAR-γ ligands, not only improve insulin resistance, but also inhibit activation of Kupffer cells[32,33] and transactivation of hepatic stellate cells,[34–36] these chemicals are believed to be suitable for prevention/treatment of hepatic inflammation and fibrogenesis in NASH. Moreover, it is suggested that PPAR-γ ligand inhibits pro-inflammatory Th1 responses whereas it enhances Th2 cytokine production, which may also ameliorate steatohepatitis. Indeed, a placebo-controlled randomized study has demonstrated the therapeutic efficacy of pioglitazone, a TZD, on NASH in terms of both metabolic and histological improve-

© 2012 The Japan Society of Hepatology

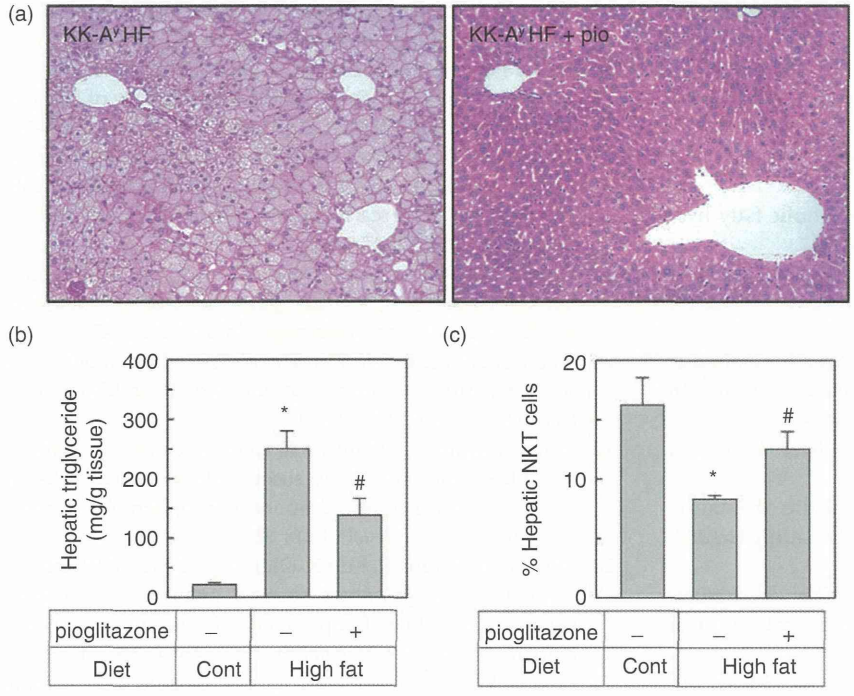

Figure 6 Pioglitazone improves HF diet-induced steatosis and expression of hepatic NKT cells in KK-A^y mice. KK-A^y mice were fed a HF diet for 4 weeks, and subsequently given repeated intragastric injections of pioglitazone for 5 days. Representative photomicrographs of liver histology from KK-A^y mice fed a HF diet (a; left panel) and pioglitazone-treated KK-A^y (a; right panel) are shown (hematoxylin–eosin, original magnification ×100). Hepatic triglyceride levels (b) and NKT cell fraction (c) were measured in KK-A^y mice fed control and HF diet with/without pioglitazone treatment ($n = 5$, mean ± SEM, $*P < 0.05$ vs control diet-fed KK-A^y, $\#P < 0.05$ vs HF diet-fed KK-A^y without pioglitazone, by ANOVA on ranks and Student–Newman–Keuls post-hoc test). HF, high fat; NKT cells, natural killer T cells; SEM, standard error of the mean.

ment.[37] Although a recent clinical trial failed to prove the significant superiority of pioglitazone over vitamin E,[38] this type of chemical is still one of the most evidenced therapeutics for NASH. In this study, we demonstrated that 5-day administration of pioglitazone restored the proportion and functional alteration of hepatic NKT cells in KK-A^y mice before and even after dietary treatment (Figs 5,6). The mechanism underlying the effect of pioglitazone on hepatic NKT cells most likely involves prevention of apoptosis in these cells (Fig. 5). Because 5-day administration of pioglitazone completely normalizes serum adiponectin levels whereas serum leptin levels remain in the high range in KK-A^y mice,[23] the expression balance of adipokines most likely play a key role in survival of NKT cells in the liver. Our data added new experimental evidence that pioglitazone restores the expression of hepatic NKT cells in metabolic syndrome-related steatohepatitis. It is therefore postulated that therapeutic effects of pioglitazone on NASH in part involve normalization of functional abnormalities in hepatic NKT cells.

In conclusion, KK-A^y mice, which present phenotypes resembling metabolic syndrome in humans, demonstrated altered expression and function of hepatic NKT cells, which most likely participate in the vulnerability to HF diet-induced steatohepatitis. Because NKT cells can produce both Th1 and Th2 cytokines, it is hypothesized that NKT cells presumably regulate Th1/Th2 balance in the liver microenvironment, thus modulating metabolic, inflammatory and tissue-repairing responses in steatohepatitis. This alteration in hepatic NKT cells in KK-A^y mice was restored by treatment with pioglitazone, most likely through normalization of adipokine expression and macrophage functions. These findings add a new aspect of therapeutic advantages of pioglitazone for the treatment of NASH.

ACKNOWLEDGMENTS

THIS WORK WAS supported in part by Grants-in-Aid (nos. 19590791 and 21590859 to K. I., no. 18390213 to S. W.) and High Technology Research Center Grant from the Ministry of Education, Culture, Sports, Science and Technology of Japan, Health and Labour Science Research Grant from the Ministry of Health, Labour and Welfare of Japan (to S. W.), and grants from Liver Forum in Kyoto (co-sponsored by Viral Hepatitis Research Foundation in Japan and Dainippon Sumitomo Pharma to K. I.), Takeda Science Foundation (to K. I.), and Research Conference on Alcohol and Health (sponsored by Suntory to K. I.) and Takeda Science Foundation (to K. I.). The authors also thank Ms Kumiko Arai (Department of

© 2012 The Japan Society of Hepatology

Gastroenterology, Juntendo University School of Medicine) for excellent technical assistance.

REFERENCES

1 Angulo P. Nonalcoholic fatty liver disease. *N Engl J Med* 2002; **346**: 1221–31.
2 Clark JM, Brancati FL, Diehl AM. Nonalcoholic fatty liver disease. *Gastroenterology* 2002; **122**: 1649–57.
3 Watanabe S, Yaginuma R, Ikejima K, Miyazaki A. Liver diseases and metabolic syndrome. *J Gastroenterol* 2008; **43**: 509–18.
4 Tilg H, Hotamisligil GS. Nonalcoholic fatty liver disease: cytokine-adipokine interplay and regulation of insulin resistance. *Gastroenterology* 2006; **131**: 934–45.
5 Li Z, Diehl AM. Innate immunity in the liver. *Curr Opin Gastroenterol* 2003; **19**: 565–71.
6 Maher JJ, Leon P, Ryan JC. Beyond insulin resistance: innate immunity in nonalcoholic steatohepatitis. *Hepatology* 2008; **48**: 670–8.
7 Gao B, Radaeva S, Park O. Liver natural killer and natural killer T cells: immunobiology and emerging roles in liver diseases. *J Leukoc Biol* 2009; **86**: 513–28.
8 Godfrey DI, MacDonald HR, Kronenberg M, Smyth MJ, Van Kaer L. NKT cells: what's in a name? *Nat Rev Immunol* 2004; **4**: 231–7.
9 Kronenberg M. Toward an understanding of NKT cell biology: progress and paradoxes. *Annu Rev Immunol* 2005; **23**: 877–900.
10 Brigl M, Brenner MB. CD1: antigen presentation and T cell function. *Annu Rev Immunol* 2004; **22**: 817–90.
11 Safadi R, Zigmond E, Pappo O, Shalev Z, Ilan Y. Amelioration of hepatic fibrosis via beta-glucosylceramide-mediated immune modulation is associated with altered CD8 and NKT lymphocyte distribution. *Int Immunol* 2007; **19**: 1021–9.
12 Ginsburg I, Koren E, Horani A *et al.* Amelioration of hepatic fibrosis via Padma Hepaten is associated with altered natural killer T lymphocytes. *Clin Exp Immunol* 2009; **157**: 155–64.
13 Park O, Jeong WI, Wang L *et al.* Diverse roles of invariant natural killer T cells in liver injury and fibrosis induced by carbon tetrachloride. *Hepatology* 2009; **49**: 1683–94.
14 Ohkawa K, Takehara T, Tatsumi T *et al.* Alterations in hepatitis B virus nucleotide sequences in a chronic virus carrier from immunotolerant to immunoactive phase. *Biochem Biophys Res Commun* 2010; **394**: 574–80.
15 Ishikawa S, Ikejima K, Yamagata H *et al.* CD1d-restricted natural killer T cells contribute to hepatic inflammation and fibrogenesis in mice. *J Hepatol* 2011; **54**: 1195–204.
16 Yang SQ, Lin HZ, Mandal AK, Huang J, Diehl AM. Disrupted signaling and inhibited regeneration in obese mice with fatty livers: implications for nonalcoholic fatty liver disease pathophysiology. *Hepatology* 2001; **34**: 694–706.
17 Picard C, Lambotte L, Starkel P *et al.* Steatosis is not sufficient to cause an impaired regenerative response after partial hepatectomy in rats. *J Hepatol* 2002; **36**: 645–52.
18 Iwatsuka H, Shino A, Suzuoki Z. General survey of diabetic features of yellow KK mice. *Endocrinol Jpn* 1970; **17**: 23–35.
19 Miller MW, Duhl DM, Vrieling H *et al.* Cloning of the mouse agouti gene predicts a secreted protein ubiquitously expressed in mice carrying the lethal yellow mutation. *Genes Dev* 1993; **7**: 454–67.
20 Masaki T, Chiba S, Tatsukawa H *et al.* Adiponectin protects LPS-induced liver injury through modulation of TNF-alpha in KK-A^y obese mice. *Hepatology* 2004; **40**: 177–84.
21 Okumura K, Ikejima K, Kon K *et al.* Exacerbation of dietary steatohepatitis and fibrosis in obese, diabetic KK-A^y mice. *Hepatol Res* 2006; **36**: 217–28.
22 Kon K, Ikejima K, Okumura K, Arai K, Aoyama T, Diabetic WS. KK-A^y mice are highly susceptible to oxidative hepatocellular damage induced by acetaminophen. *Am J Physiol Gastrointest Liver Physiol* 2010; **299**: G329–37.
23 Aoyama T, Ikejima K, Kon K, Okumura K, Arai K, Watanabe S. Pioglitazone promotes survival and prevents hepatic regeneration failure after partial hepatectomy in obese and diabetic KK-A^y mice. *Hepatology* 2009; **49**: 1636–44.
24 Li Z, Soloski MJ, Diehl AM. Dietary factors alter hepatic innate immune system in mice with nonalcoholic fatty liver disease. *Hepatology* 2005; **42**: 880–5.
25 Dumas ME, Barton RH, Toye A *et al.* Metabolic profiling reveals a contribution of gut microbiota to fatty liver phenotype in insulin-resistant mice. *Proc Natl Acad Sci USA* 2006; **103**: 12511–6.
26 DiBaise JK, Zhang H, Crowell MD, Krajmalnik-Brown R, Decker GA, Rittmann BE. Gut microbiota and its possible relationship with obesity. *Mayo Clin Proc* 2008; **83**: 460–9.
27 Thurman RG II. Alcoholic liver injury involves activation of Kupffer cells by endotoxin. *Am J Physiol* 1998; **275**: G605–11.
28 Wigg AJ, Roberts-Thomson IC, Dymock RB, McCarthy PJ, Grose RH, Cummins AG. The role of small intestinal bacterial overgrowth, intestinal permeability, endotoxaemia, and tumour necrosis factor alpha in the pathogenesis of non-alcoholic steatohepatitis. *Gut* 2001; **48**: 206–11.
29 Li Z, Yang S, Lin H *et al.* Probiotics and antibodies to TNF inhibit inflammatory activity and improve nonalcoholic fatty liver disease. *Hepatology* 2003; **37**: 343–50.
30 Miele L, Valenza V, La Torre G *et al.* Increased intestinal permeability and tight junction alterations in nonalcoholic fatty liver disease. *Hepatology* 2009; **49**: 1877–87.
31 Michalik L, Wahli W. Involvement of PPAR nuclear receptors in tissue injury and wound repair. *J Clin Invest* 2006; **116**: 598–606.
32 Uchimura K, Nakamuta M, Enjoji M *et al.* Activation of retinoic X receptor and peroxisome proliferator-activated receptor-gamma inhibits nitric oxide and tumor necrosis factor-alpha production in rat Kupffer cells. *Hepatology* 2001; **33**: 91–9.

© 2012 The Japan Society of Hepatology

33 Enomoto N, Takei Y, Hirose M *et al.* Prevention of ethanol-induced liver injury in rats by an agonist of peroxisome proliferator-activated receptor-gamma, pioglitazone. *J Pharmacol Exp Ther* 2003; **306:** 846–54.
34 Miyahara T, Schrum L, Rippe R *et al.* Peroxisome proliferator-activated receptors and hepatic stellate cell activation. *J Biol Chem* 2000; **275:** 35715–22.
35 Kon K, Ikejima K, Hirose M *et al.* Pioglitazone prevents early-phase hepatic fibrogenesis caused by carbon tetrachloride. *Biochem Biophys Res Commun* 2002; **291:** 55–61.
36 Galli A, Crabb DW, Ceni E *et al.* Antidiabetic thiazolidinediones inhibit collagen synthesis and hepatic stellate cell activation *in vivo* and *in vitro*. *Gastroenterology* 2002; **122:** 1924–40.
37 Belfort R, Harrison SA, Brown K *et al.* A placebo-controlled trial of pioglitazone in subjects with nonalcoholic steatohepatitis. *N Engl J Med* 2006; **355:** 2297–307.
38 Sanyal AJ, Chalasani N, Kowdley KV *et al.* Pioglitazone, vitamin E, or placebo for nonalcoholic steatohepatitis. *N Engl J Med* 2010; **362:** 1675–85.

© 2012 The Japan Society of Hepatology

Am J Physiol Gastrointest Liver Physiol 304: G293–G299, 2013.
First published October 18, 2012; doi:10.1152/ajpgi.00083.2012.

Innate immune responses involving natural killer and natural killer T cells promote liver regeneration after partial hepatectomy in mice

Satoko Hosoya,[1] Kenichi Ikejima,[1] Kazuyoshi Takeda,[2] Kumiko Arai,[1] Sachiko Ishikawa,[1] Hisafumi Yamagata,[1] Tomonori Aoyama,[1] Kazuyoshi Kon,[1] Shunhei Yamashina,[1] and Sumio Watanabe[1]

[1]*Department of Gastroenterology, Juntendo University Graduate School of Medicine, Tokyo, Japan; and* [2]*Department of Immunology, Juntendo University Graduate School of Medicine, Tokyo, Japan*

Submitted 29 February 2012; accepted in final form 7 October 2012

Hosoya S, Ikejima K, Takeda K, Arai K, Ishikawa S, Yamagata H, Aoyama T, Kon K, Yamashina S, Watanabe S. Innate immune responses involving natural killer and natural killer T cells promote liver regeneration after partial hepatectomy in mice. *Am J Physiol Gastrointest Liver Physiol* 304: G293–G299, 2013. First published October 18, 2012; doi:10.1152/ajpgi.00083.2012.—To clarify the roles of innate immune cells in liver regeneration, here, we investigated the alteration in regenerative responses after partial hepatectomy (PH) under selective depletion of natural killer (NK) and/or NKT cells. Male, wild-type (WT; C57Bl/6), and CD1d-knockout (KO) mice were injected with anti-NK1.1 or anti-asialo ganglio-*N*-tetraosylceramide (GM1) antibody and then underwent the 70% PH. Regenerative responses after PH were evaluated, and hepatic expression levels of cytokines and growth factors were measured by real-time RT-PCR and ELISA. Phosphorylation of STAT3 was detected by Western blotting. Depletion of both NK and NKT cells with an anti-NK1.1 antibody in WT mice caused drastic decreases in bromodeoxyuridine uptake, expression of proliferating cell nuclear antigen, and cyclin D1, 48 h after PH. In mice given NK1.1 antibody, increases in hepatic TNF-α, IL-6/phospho-STAT3, and hepatocyte growth factor (HGF) levels following PH were also blunted significantly, whereas IFN-γ mRNA levels were not different. CD1d-KO mice per se showed normal liver regeneration; however, pretreatment with an antiasialo GM1 antibody to CD1d-KO mice, resulting in depletion of both NK and NKT cells, also blunted regenerative responses. Collectively, these observations clearly indicated that depletion of both NK and NKT cells by two different ways results in impaired liver regeneration. NK and NKT cells most likely upregulate TNF-α, IL-6/STAT3, and HGF in a coordinate fashion, thus promoting normal regenerative responses in the liver.

innate immunity; TNF-α; IL-6; STAT3; hepatocyte growth factor

LINES OF EVIDENCE HAVE SUGGESTED that alteration in the innate immune system is involved in a variety of pathophysiological conditions in the liver (24). It is well known that the liver contains a variety of immune cells, with a considerable proportion of natural killer (NK) and NKT cell fractions (6). NK cells are defined as large, granular lymphocytes that exert cytotoxic activity against tumors and viral-infected cells through the perforin and granzyme systems (27). NK cells preferentially reside in the hepatic sinusoid, and these liver-specific NK cells are called Pit cells (31). On the other hand, NKT cells are a heterogeneous subset of lymphocytes expressing both NK and T cell surface markers (8, 14). NKT cells recognize a glycolipid antigen presented by CD1d, one of the major histocompatibility complex molecules, on antigen-presenting cells, such as dendritic cells and macrophages (3, 8). Several studies suggested that NKT cells modulate hepatic inflammation and fibrogenesis (7, 12, 21, 23, 25); however, the precise role of these cells in liver pathophysiology is still controversial.

Liver regeneration is one of the significant natures of this important organ. The normal liver is capable of regenerating when injured by various pathogens and mechanical damages (20, 29). The mechanism underlying this process has been studied from various aspects; however, it still remains unclear. Recent lines of evidence indicated that innate immune responses play a key role in the trigger and promotion of the regenerating process (5). For example, pattern-recognition receptors, such as Toll-like receptors, and downstream signaling involved in production of cytokines from hepatic macrophages (Kupffer cells) are quite important in liver regeneration (11, 26). However, the role of other types of innate immune cells, such as NK and NKT cells, in liver regeneration has not been fully elucidated. A recent report indicated that NK cells negatively regulate liver regeneration through production of IFN-γ (28). The role of NKT cells in liver regeneration is more obscure; poor regeneration in steatotic liver in ob/ob mice has been reported (16, 32), where hepatic NKT cells are depleted (17). Similarly, we have shown recently that KK-A^y mice, which develop a metabolic, syndrome-like phenotype spontaneously, demonstrate poor regeneration following 70% partial hepatectomy (PH) (2), where hepatic NKT cells are also depleted. Furthermore, activation of NKT cells triggered by a specific ligand α-galactosylceramide has been shown to accelerate liver regeneration after PH (22). These observations suggested that NKT cells promote the regeneration process; however, mice lacking NKT cells caused by genetic knockout (KO) of CD1d have been shown to demonstrate almost normal liver regeneration after PH (28).

In the present study, we therefore investigated the role of hepatic NK and NKT cells in liver regeneration following PH using mice lacking NK and/or NKT cells generated by a combination of KO animals and selective depletion of these cells by specific antibodies.

MATERIALS AND METHODS

Animal experiments. Male, wild-type (WT) C57Bl/6 mice, 7 wk after birth, were obtained from CLEA Japan (Tokyo, Japan). A colony of CD1d-KO mice raised from the C57Bl/6 strain (a generous gift from the Department of Immunology, Juntendo University of Medicine, Tokyo, Japan) was maintained in the animal facility in our institution—Juntendo University Graduate School of Medicine (9, 19). All animals received humane care in compliance with the experimental protocol approved by the Committee of Laboratory Animals, according to institutional guidelines. Mice were housed in air-condi-

Address for reprint requests and other correspondence: K. Ikejima, Dept. of Gastroenterology, Juntendo Univ. Graduate School of Medicine, 2-1-1 Hongo, Bunkyo-ku, Tokyo, 113-8421 Japan (e-mail: ikejima@juntendo.ac.jp).

 0193-1857/13 Copyright © 2013 the American Physiological Society

tioned, specific pathogen-free animal quarters with lighting from 0800 to 2000 and were given unrestricted access to standard lab chow and water for 1 wk prior to experiments. After overnight fasting, 70% PH was performed in the mice, according to the Higgins and Anderson method (10). Some mice were given a single intraperitoneal injection of a mouse anti-NK1.1 MAb (PK136; 150 μg/body; provided by the Department of Immunology, Juntendo University School of Medicine) or an anti-asialo ganglio-*N*-tetraosylceramide (GM1) antibody (200 μg/body; provided by the Department of Immunology, Juntendo University School of Medicine), 24 h prior to operation. For the extended time course over 72 h following PH, mice were given the second injection of antibodies at 48 h after PH. Mice were killed by exsanguination from inferior vena cava, and serum and liver samples were obtained. Some mice were pulse labeled with a single intraperitoneal injection of bromodeoxyuridine (BrdU; Sigma Chemical, St. Louis, MO; 50 mg/kg in PBS), 2 h prior to death, and liver specimens were fixed in buffered formalin for immunohistochemistry. Serum and liver samples were kept frozen at −80°C until assayed.

Immunohistochemistry. For immunohistochemistry, formalin-fixed and paraffin-embedded tissue sections were deparaffinized and incubated with 3% H_2O_2 for 10 min. To examine BrdU incorporation to hepatocyte nuclei, tissue sections were incubated with 2 N HCl for 30 min. After blocking with normal horse serum for 60 min, tissue sections were incubated with a mouse anti-BrdU MAb (DakoCytomation Norden A/S, Glostrup, Denmark). After rinsing the primary antibody, the sections were incubated with secondary biotinylated antimouse IgG antibody, and specific binding was visualized with avidin-biotin complex solution, followed by incubation with a 3,3-diaminobenzidine tetrahydrochloride solution using the Vectastain Elite ABC kit (Vector Laboratories, Burlingame, CA). BrdU-positive hepatocytes were counted in five 100× fields on each slide to determine the average number BrdU-labeling index (BrdU-positive hepatocytes/total hepatocytes). Expression of proliferating cell nuclear antigen (PCNA) in hepatocytes was evaluated similarly by immunohistochemistry as described previously elsewhere (1). Specimens were observed and photographed using a microscope equipped with a digital imaging system (Leica DM 2000; Leica Microsystems GmbH, Germany).

Western blot analysis. Whole liver protein extracts were prepared by homogenizing frozen tissue in a buffer containing 50 mM Tris-HCl (pH 8.0), 150 mM NaCl, 1 mM EDTA, 1% Triton X-100, protease inhibitors (cOmplete, mini protease inhibitor cocktail tablets; Roche Diagnostics, Mannheim, Germany), and a phosphatase inhibitor Na_3VO_4 (50 μM; Sigma Chemical), followed by centrifugation at 15,000 rpm for 10 min. Protein concentration was determined by Bradford assay using the Bio-Rad protein assay kit (Bio-Rad Laboratories, Hercules, CA). Twenty micrograms of protein was separated in 10% SDS-PAGE and electrophoretically transferred onto polyvinylamide fluoride membranes. After blocking with 5% nonfat dry milk in Tris-buffered saline, membranes were incubated overnight at 4°C with rabbit polyclonal anticyclin D1 or antiphospho-STAT3 (Tyr705; Cell Signaling Technology, Beverly, MA), followed by a secondary horseradish peroxidase-conjugated antirabbit IgG antibody (DakoCytomation Norden A/S). Subsequently, specific bands were visualized using the enhanced chemiluminescence detection kit (GE Healthcare, Buckinghamshire, UK). Images were captured using a lumino-image analyzer (LAS-3000; Fujifilm, Tokyo, Japan), and densitometry was performed using Multi Gauge software (Fujifilm).

ELISA. Hepatocyte growth factor (HGF) levels in the liver homogenate were determined using an ELISA kit (Institute of Immunology, Tokyo, Japan), according to the manufacturer's instruction. Serum IL-6 levels were measured similarly by an ELISA kit (R&D Systems, Minneapolis, MN).

Cell culture. Hepatic stellate cell (HSC)-T6 cells, a rat HSC line, were cultured on polystyrene dishes using DMEM (Invitrogen, Carlsbad, CA), supplemented with 10% FBS in a humidified air containing 5% CO_2 at 37°C. Cells were then incubated with recombinant murine IFN-γ, TNF-α, IL-4, or IL-13 (10 ng/ml each; R&D Systems) for 3–6 h as appropriate.

RNA preparation and real-time RT-PCR. Total RNA was prepared from frozen tissue samples or culture cells using the illustra RNAspin Mini RNA Isolation kit (GE Healthcare). The concentration and purity of isolated RNA were determined by measuring optical density at 260 and 280 nm. Furthermore, the integrity of RNA was verified by electrophoresis on formaldehyde-denaturing agarose gels.

For real-time RT-PCR, total RNA (1 μg) was reverse transcribed using Moloney murine leukemia virus transcriptase (SuperScript II, Invitrogen) and an oligo(dT) 12–18 primer (Invitrogen) at 42°C for 1 h. Obtained cDNA (1 μg) was amplified using SYBR Premix Ex Taq (Takara Bio, Tokyo, Japan) and specific primers for IFN-γ, TNF-α, HGF, IL-4, IL-6, suppressor of cytokine signal (SOCS)-3, and GAPDH, as appropriate (Table 1). After a 10-s activation period at 95°C, 40 cycles of 95°C for 5 s and 60°C for 31 s, followed by the final cycle of 95°C for 15 s, 60°C for 1 min, and 95°C for 15 s, were performed using the ABI PRISM 7700 sequence detection system (PE Applied Biosystems, Foster City, CA), and the threshold cycle values were obtained.

Statistical analysis. Data were expressed as means ± SE. Statistical differences between means were determined using two-way ANOVA or ANOVA on ranks, followed by a post hoc test (Student-Newman-Keuls all pairwise comparison procedures) as appropriate. A value of $P < 0.05$ was selected before the study to reflect significance.

Table 1. *Primer sets for real-time RT-PCR*

Gene (GeneBank Accession)	Primer Sequences	Product Size
IFN-γ (NM_008337.3)	forward: 5′-CGGCACAGTCATTGAAAGCCTA-3′ reverse: 5′-GTTGCTGATGGCCTGATTGTC-3′	199 bp
TNF-α (NM_013693.2)	forward: 5′-AAGCCTGTAGCCCACGTCGTA-3′ reverse: 5′-GGCACCACTAGTTGGTTGTCTTTG-3′	122 bp
HGF (NM_010427.4)	forward: 5′-AGAAATGCAGTCAGCACCATCAAG-3′ reverse: 5′-GATGGCACATCCACGACCAG-3′	179 bp
IL-4 (NM_021283.2)	forward: 5′-ACGGAGATGGATGTGCCAAAC-3′ reverse: 5′-AGCACCTTGGAAGCCCTACAGA-3′	83 bp
IL-6 (NM_031168.1)	forward: 5′-CCACTTCACAAGTCGGAGGCTTA-3′ reverse: 5′-GCAAGTGCATCATCGTTGTTCATAC-3′	112 bp
SOCS-3 (NM_007707)	forward: 5′-CAATACCTTTGACAAGCGGACTCTC-3′ reverse: 5′-TCAAAGCGCAAACAAGTTCCAG-3′	146 bp
GAPDH (NM_008084.2)	forward: 5′-TGTGTCCGTCGTGGATCTGA-3′ reverse: 5′-TTGCTGTTGAAGTCGCAGGAG-3′	150 bp

HGF, hepatocyte growth factor; SOCS-3, suppressor of cytokine signal-3.

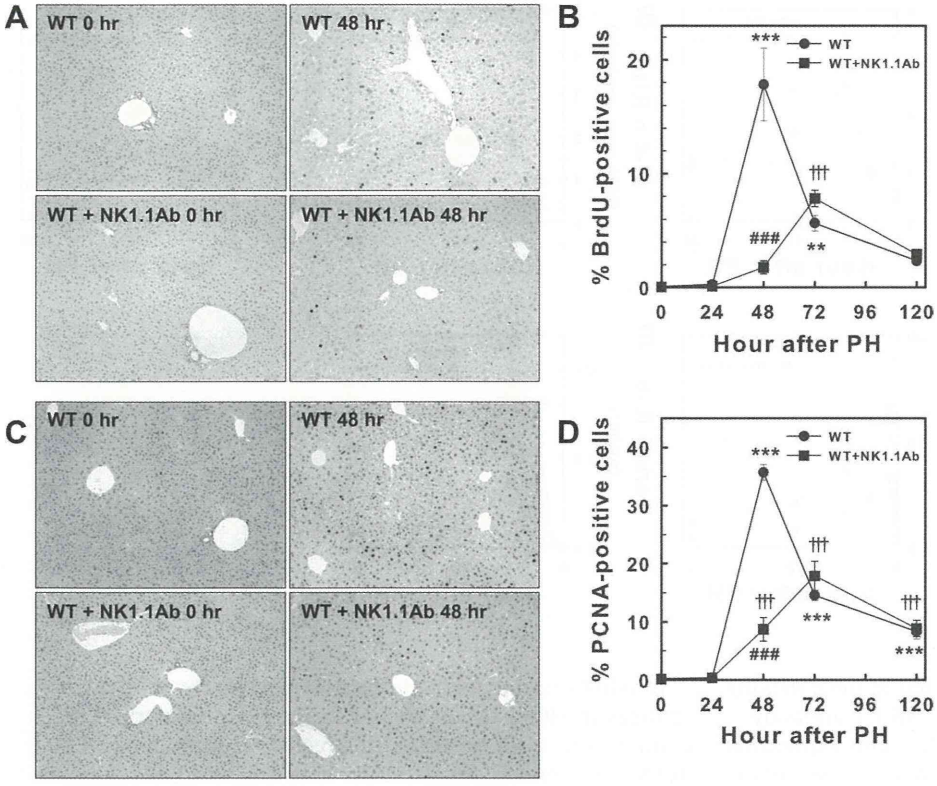

Fig. 1. Anti-NK1.1 antibody inhibits liver regeneration after partial hepatectomy (PH). Wild-type (WT) mice were given a single injection of an anti-NK1.1 antibody (Ab; 150 μg/body), 24 h before PH. Representative photomicrographs of immunohistochemistry for bromodeoxyuridine (BrdU; *A*) and proliferating cell nuclear antigen (PCNA; *C*), before and 48 h after PH, are shown (original magnification: ×100). The average labeling indices for BrdU (*B*) and PCNA (*D*) for WT controls (●) and anti-NK1.1 antibody-treated WT (■) after PH are plotted ($n = 5$; $^{**}P < 0.01$; $^{***}P < 0.001$ vs. WT before PH; †††$P < 0.001$ vs. antibody-treated WT before PH; ###$P < 0.001$ vs. WT at the same time point).

RESULTS

Liver regeneration is impaired in mice pretreated with anti-NK1.1 antibody. To evaluate the role of NK and NKT cells in liver regeneration, we first tried to evaluate the alteration in hepatic regeneration following 70% PH in mice pretreated with a mouse anti-NK1.1 MAb (PK136). A single intraperitoneal injection of this antibody caused depletion of both NK and NKT cells in the liver almost completely for at least 3 days, which was confirmed by fluorescence-activated cell sorting analysis (data not shown). Male C57Bl/6 mice (WT), 8 wk after birth, were pretreated with this antibody and underwent 70% PH 24 h later. BrdU uptake into hepatocyte nuclei was observed 48 h after PH (Fig. 1*A*). In the control C57Bl/6 mice, the percentages of BrdU-positive hepatocytes reached nearly 20% as expected; however, pretreatment with an anti-NK1.1 antibody drastically blunted this increase (Fig. 1*B*). Similarly, increases in PCNA-positive hepatocytes, 48 h after PH, were blunted largely by pretreatment with an anti-NK1.1 antibody (Fig. 1*C*), the values reaching only 40% of control values (Fig. 1*D*). To determine whether delayed regeneration occurs in the late phase, we observed an extended time course with the second injection of an anti-NK1.1 antibody at 48 h after PH. At *day 5* after PH, all animals were surviving, and the liver/body wt ratio in NK1.1 antibody-treated mice reached 94% of those without NK1.1 antibody treatment, clearly indicating that depletion of NK and NKT cells retards but does not irreversibly impair the regenerating process.

Furthermore, we detected the hepatic expression of cyclin D1 following PH by Western blotting (Fig. 2*A*). The hepatic expression levels of cyclin D1 were peaked at 48 h after PH in control mice as expected; however, the levels in mice pretreated with an anti-NK1.1 antibody only reached one-fifth of controls at the same time point (Fig. 2*B*). Whereas the expression levels of cyclin D1 in WT mice were decreased after the peak at 48 h, the levels in anti-NK1.1 antibody-treated mice were increased gradually in 72 h after PH, indicating that the regenerative process is indeed retarded by pretreatment with an anti-NK1.1 antibody. Taken together, these findings clearly

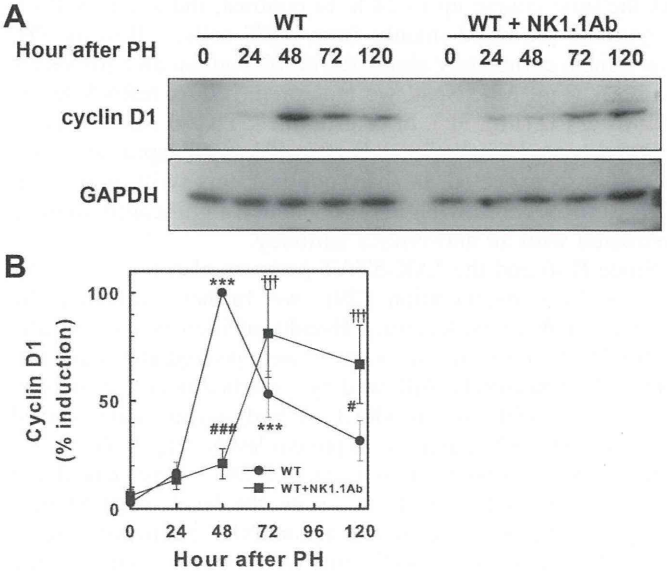

Fig. 2. Anti-NK1.1 antibody blunts induction of cyclin D1 after PH. Representative photographs of Western blotting for hepatic cyclin D1 (*A*) and densitometrical data (*B*) for WT controls (●) and anti-NK1.1 antibody-treated WT (■) are shown ($n = 5$; $^{***}P < 0.001$ vs. WT before PH; †††$P < 0.001$ vs. antibody-treated WT before PH; #$P < 0.05$; ###$P < 0.001$ vs. WT at the same time point).

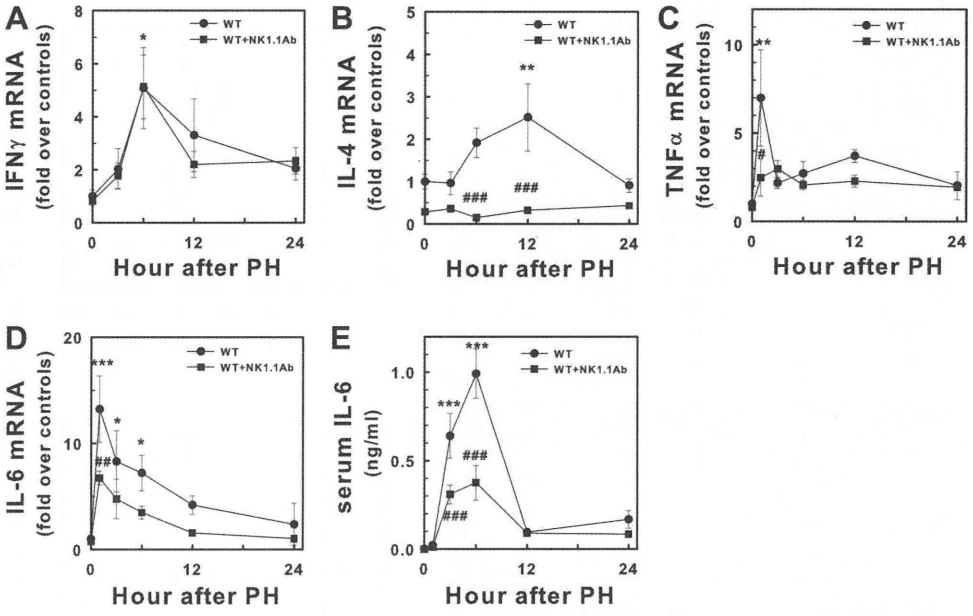

Fig. 3. Cytokine expression following PH in mice pretreated with an anti-NK1.1 antibody. Steady-state mRNA levels for IFN-γ, IL-4, TNF-α, and IL-6 in the liver were measured by real-time RT-PCR, and serum IL-6 levels were measured by ELISA. Average values of IFN-γ (*A*), IL-4 (*B*), TNF-α (*C*), and IL-6 (*D*) mRNA levels and serum IL-6 levels (*E*) in WT (●) and anti-NK1.1 antibody-treated WT (■) are plotted ($n = 5$; $^{*}P < 0.05$; $^{**}P < 0.01$; $^{***}P < 0.001$ vs. WT before PH; $\#P < 0.05$; $\#\#P < 0.01$; $\#\#\#P < 0.001$ vs. WT at the same time point).

indicated that hepatic regeneration is impaired in mice lacking both NK and NKT cells caused by an anti-NK1.1 antibody.

Pretreatment with an anti-NK1.1 antibody blunts expression of cytokines and growth factors triggering liver regeneration. We then evaluated the induction of cytokines affecting regenerative responses following PH. Since IFN-γ produced from NK cells has been demonstrated to downregulate the liver regeneration process (28), we first evaluated the hepatic expression of IFN-γ mRNA in mice pretreated with an anti-NK1.1 antibody (Fig. 3*A*). In control mice, the hepatic expression levels of IFN-γ mRNA were elevated in 6 h after PH, followed by a gradual decrease. The pretreatment with an anti-NK1.1 antibody, however, did not alter the levels throughout the time course up to 24 h. In contrast, induction of IL-4, a cytokine produced mainly from NKT cells, following PH, was almost completely abolished in mice given an anti-NK1.1 antibody (Fig. 3*B*). Next, we measured TNF-α mRNA levels following PH (Fig. 3*C*). In control mice, TNF-α mRNA levels were increased markedly, 1 h after PH, with rapid decreases thereafter as expected. In sharp contrast, this swift increase in TNF-α mRNA following PH was blunted significantly in mice pretreated with an anti-NK1.1 antibody.

Since IL-6 and the JAK-STAT pathway also play a pivotal role in liver regeneration (29), we further evaluated the changes in these molecules. PH-induced increases in hepatic IL-6 mRNA and serum IL-6 levels were peaked at 1 h and 6 h after PH, respectively, followed by a gradual decrease in 24 h. Pretreatment with an anti-NK1.1 antibody significantly blunted IL-6, both in mRNA and serum protein levels (Fig. 3, *D* and *E*). Furthermore, phosphorylation levels of STAT3 were peaked at 3 h after PH in WT controls; however, the levels were blunted markedly in mice pretreated with an anti-NK1.1 antibody (Fig. 4, *A* and *B*). Moreover, hepatic mRNA levels of SOCS-3, the downstream inhibitory molecules of the JAK-STAT pathway, were also blunted significantly (Fig. 4*C*). Taken together, these findings clearly indicated that IL-6 and JAK-STAT signaling following PH were thoroughly downregulated by pretreatment with an anti-NK1.1 antibody.

In addition to cytokine responses, we further evaluated the changes in HGF, which plays a key role in the normal regenerating process in the liver. Interestingly, elevations in HGF mRNA and protein levels in the liver following PH were also blunted significantly (Fig. 5, *A* and *B*). Since one of the major sources of HGF is HSCs, we evaluated whether cytokines derived from NK and NKT cells elicit HGF production in vitro using HSC-T6 cells. Indeed, steady-state mRNA levels of HGF were significantly elevated in HSC-T6 cells following incubation with IFN-γ, TNF-α, IL-4, and IL-13 (Fig. 5*C*). Collectively, these findings indicated that pretreatment with an anti-

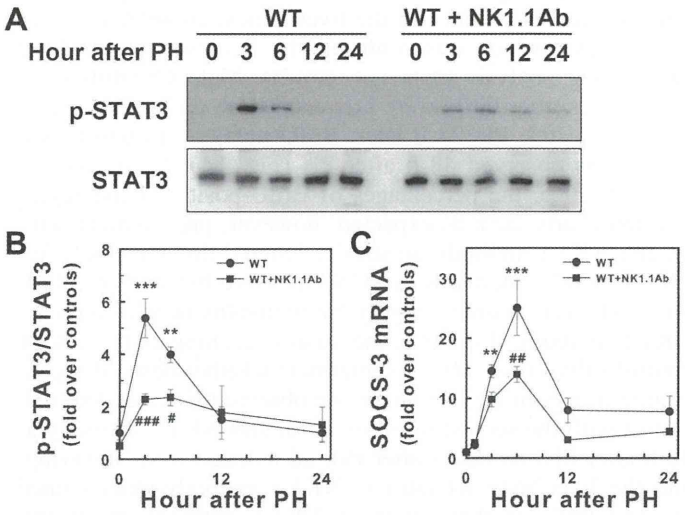

Fig. 4. Phosphorylation of STAT3 (p-STAT3) and expression of suppressor of cytokine signal (SOCS)-3 following PH in mice pretreated with an anti-NK1.1 antibody. p-STAT3 was detected by Western blotting. Steady-state mRNA levels for SOCS-3 were determined by real-time RT-PCR. Representative photographs of specific bands for p-STAT3 in WT and WT pretreated with an anti-NK1.1 antibody are shown (*A*). Densitometrical data for p-STAT3/STAT3 (*B*) and average expression levels of SOCS-3 mRNA (*C*) are plotted ($n = 5$; $^{**}P < 0.01$; $^{***}P < 0.001$ vs. WT before PH; $\#P < 0.05$; $\#\#P < 0.01$; $\#\#\#P < 0.001$ vs. WT at the same time point).